High-yield seeded growth of monodisperse pentatwinned gold nanoparticles through thermally induced seed twinning

High Yield Seeded Growth of Monodisperse Pentatwinned Gold Nanoparticles Through Thermally-Induced Seed Twinning.

Ana Sánchez-Iglesias† , Naomi Winckelmans‡ , Thomas Altantzis‡ , Sara Bals‡ , Marek Grzelczak†‖ * , Luis M. Liz-Marzán†‖ §*

† Bionanoplasmonics Laboratory, CICbiomaGUNE, Paseo de Miramón 182, 20014 Donostia – San Sebastián, Spain

‡ EMAT-University of Antwerp, Groenenborgerlaan 171, B-2020 Antwerp, Belgium

‖ Ikerbasque, Basque Foundation for Science, 48013 Bilbao, Spain

§ Ciber de Bioingeniería, Biomateriales y Nanomedicina, Ciber-BBN, 20014 Donostia – San Sebastián, Spain

KEYWORDS Gold Nanoparticles, Twin planes, bipyramids, nanorods, decahedra, seeds

ABSTRACT: We show here that thermal treatment of small seeds results in extensive twinning and a subsequent drastic yield improvement (>85%) in the formation of pentatwinned nanoparticles, with pre-selected morphology (nanorods, bipyramids and decahedra) and aspect ratio. The "quality" of the seeds thus defines the yield of the obtained nanoparticles, which in the case of nanorods avoids the need for additives such as Ag+ ions. This modified seeded growth method also improves reproducibility, as the seeds can be stored for extended periods of time without compromising the quality of the final nanoparticles. Additionally, minor modification of the seeds with Pd allows their localization within the final particles, which opens new avenues toward mechanistic studies. All together, these results represent a paradigm shift in anisotropic gold nanoparticle synthesis.

Although recent progress of seeded-growth has made available an extensive library of anisotropic metal nanoparticles,[1–4] the chemical complexity of the growth solution, often involving organic additives,[5] and the structural instability of the seeds hinder the quest for high quality products. For the sake of synthetic simplicity, merging different synthetic protocols by finding common growth routes, is a mandatory step to reach a universal growth mechanism[6] and reproducible fabrication. The family of pentatwinned gold nanoparticles (decahedra, rods, and bipyramids) is a typical example of nanostructures suffering from low synthetic yield, which has hindered their potential for practical applications. More specifically, the reported yields for decahedra,[7] rods[8] and bipyramids[9,10] can reach 35%, 30% and 60%, respectively. It has been proposed that the reason for such low yields is the poor control over the crystal habit of the seeds, which ultimately determines the crystallinity and shape of the resulting nanoparticles.[11] Postsynthesis purification methods can largely improve the yield of the desired nanoparticle morphology,[12–14] but they are usually tedious, time-consuming and thus impractical for largescale production. Additionally, current seeded growth methods have limited reproducibility, in part because the seeds gradually change with time, resulting in uncontrolled differences in the final product.[15]

We report here a seed optimization protocol that leads to extensive twinning, which in turns drives a dramatic increase in the seeded growth yield of gold nanorods, bipyramids and decahedra. The synthesis starts with a mild thermal treatment of common seeds, in the presence of a cationic surfactant (cetyl-trimethylammonium bromide, CTAB) and sodium citrate. Upon heating, a slight increase in the average particle size was appreciated, along with a gradual increase in the

percentage of twinned seeds with heating time. Once produced, the resulting seeds are stable, meaning that they can be stored for extended periods of time without affecting the ultimate quality of the obtained nanoparticles, i.e. the reproducibility of seeded growth is also largely improved as compared to the conventional seeded-growth approach. Finally, the longterm stability of the seeds permits post-synthetic doping with other metals (e.g. palladium), which serve as markers for spatial localization of the seeds within the final particles.

Our central hypothesis originated from the commonly accepted statement that the crystal structure of the seeds defines the crystallinity of the final nanoparticles.[11,16] Thus, if twin planes can be introduced in the seeds, available protocols could be directly implemented for the seeded growth of either decahedra, rods, or bipyramids. In other words, we hypothesized that by increasing the population of twinned nanoparticles in the seed solution we should enhance the yield of twinned particles.

We devised a novel protocol for the preparation of Au seeds that builds up from recent reports,10,11 in which $NaBH_4$ is used to reduce $HAuCl_4$, in the presence of both CTAC and citric acid. Details can be found in the Supporting Information. The as-prepared seed solution was brownish and displayed no localized surface plasmon resonance (LSPR) band (Figure1a,b), suggesting that the seed diameter is kept below 2 nm.[11] Heating up the seed solution at 80 ºC was found to be the key step, leading to a gradual color change from brown to red, indicative of increased particle size (Figure 1a). Time-resolved UV-Vis spectroscopy monitoring of the seed solution (Figure 1b) confirmed the emergence of a narrow LSPR band (529 nm), with increasing intensity until reaching a constant absorbance after 90 min. TEM analysis of the treated colloid confirmed the growth of monodisperse nanoparticles, with an average diameter of 6.1 ± 0.2 nm (Figure 1c). The crystal habit of the thermally treated seeds was studied by Annular Dark Field Scanning Transmission Electron Microscopy (ADFSTEM) at relatively low magnification and high camera length. By inspection of the residual diffraction contrast in 200 different nanoparticles (see representative images in Figure S1), we concluded that 91% of the particles were twinned. To obtain more detailed information concerning the number of twins in the individual particles, high resolution High Angle Annular Dark Field Scanning Transmission Electron Microscopy (HAADF-STEM) measurements were performed on 35 twinned particles. The analysis revealed that 89% of the particles are pentatwinned, whereas the remaining 11% contain one or more twin planes. An example for each type of particle is presented in Figure 1d, with red arrows indicating the twin planes. This result clearly indicates that the thermal treatment induces not only growth but also twin formation in the nanoparticle seeds.

As a first example of seeded growth from thermally treated seeds, we implemented the experimental conditions developed by Liu and Guyot-Sionnest11 for the synthesis of Au bipyramids, which involved the use of a growth solution containing $AgNO_3$, CTAB, ascorbic acid, and $HAuCl_4$ (details in Supporting Information). In order to evaluate the effect of thermal treatment, we synthesized bipyramids from gold seeds heated for different times (0, 10, 20, 30, 60 and 90 min; 80 ºC). As shown in Figure 2a, longer aging times led to more intense and blue-shifted longitudinal LSPR, while the band at ~500 nm gradually damped

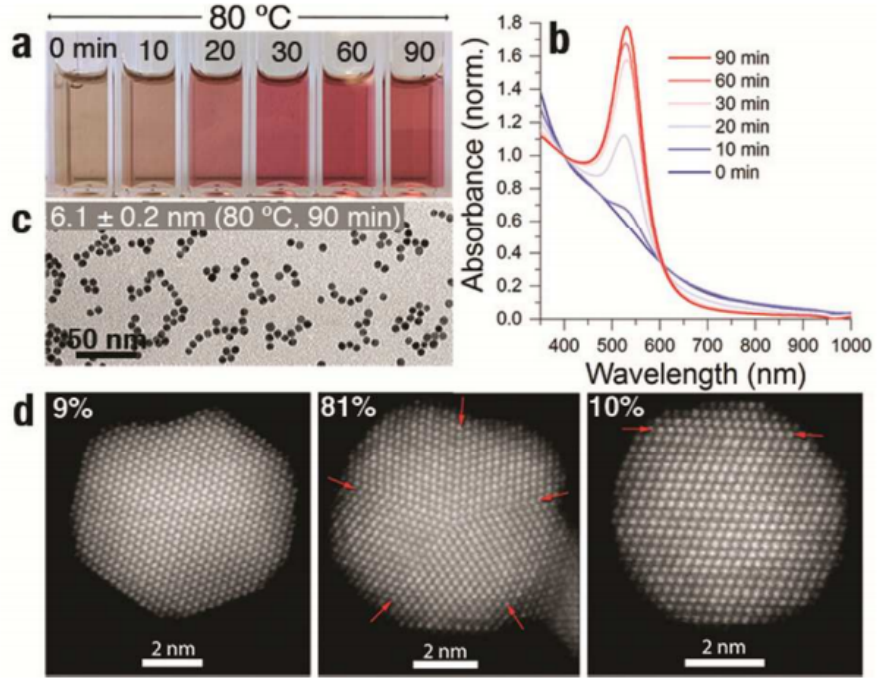

Figure 1. Thermally-induced twinning in gold seeds. (a) Images of seed solution thermally treated for different times as labeled. (b) Time-resolved UV-Vis spectra of the heated seed solution. (c) Representative TEM image of the seeds treated for 90 minutes at 80 ºC. (d) HAADF-STEM images of the three types of seeds after thermal treatment for 90 min, and their relative distribution. Red arrows indicate twin planes.

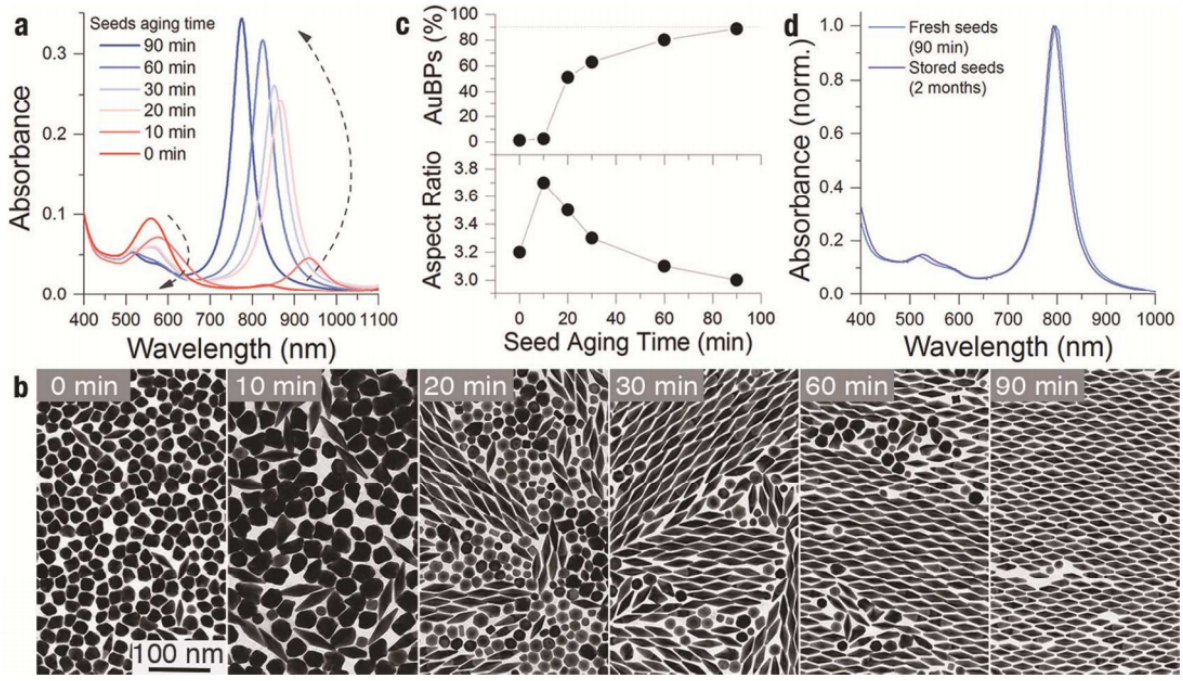

Figure 2. Effect of seed thermal treatment on the yield of bipyramids. (a) UV-Vis-NIR spectra of samples prepared using seeds at different heating times. (b) TEM images of the same samples as in (A). (c) Percentage of bipyramids and average aspect ratio vs. seed heating time (d) Spectra of samples prepared with the same seeds, right after heating and stored for 2 months.

Such changes indicate the formation of bipyramids with different aspect ratios and increasing shape yield (lower amount of spheres). TEM analysis confirmed the gradual enrichment of bipyramids (Figure 2b and Figures S2-S7), ranging from ca. 1% to 85%, between 0 and 90 minutes of thermal treatment (Figure 2c). Interestingly, the limiting yield of the synthesis correlated with the population of twinned seeds, as determined by TEM analysis (counting >5000 particles), confirming that the use of seeds containing twin planes dictated the growth of twinned nanoparticles.
The thermal aging process involves structural and morphological changes in the seeds. For shorter aging times (from 0 and 10 min), the resulting fraction of bipyramids increased only from 1.2% to 2.4%, while the aspect ratio increased drastically from 3.2 to 3.8 (Figure 2c). We conclude that at short aging times the seeds become bigger but without significant twin formation. At aging times above 10 min, the yield of bipyramids steadily increased up to 85-90% after 90 min, while the aspect ratio decreased to 3.0, meaning that seed twinning became dominant. We propose that the interplay between structural (twin) and morphological (size) changes can be further tuned via experimental parameters such as temperature, citric acid concentration or the presence of other organic additives.
The formation of twin planes in the seeds during the thermal process requires the presence of citric acid (5 mM) and CTAC (50 mM). Although both species bind to metal surface, citrate ions are known to induce twin defect formation.17 Hindering the access of citrate ions to gold seeds by replacing CTAC by CTAB (bromide has a stronger binding energy to gold than chloride) during the thermal treatment, was found to hinder the quality of the obtained bipyramids (Figure S8). A similar effect was observed when using CTAC only (no citric acid) during thermal treatment (Figure S8). An additional advantage of thermally treated seeds is their structural stability over extended periods of time, which is clearly demonstrated by repeating the synthesis of bipyramids using the same seed solution after storage for two months under ambient conditions. The spectrum of the resulting colloid showed perfect overlap with that of a sample grown from freshly prepared seeds (Figure 2d and Figure S9). Such a striking reproducibility represents a significant advantage over existing synthetic methods, since seed preparation (nucleation) can be fully decoupled from (seeded) growth.
We next show the general application of thermally treated seeds to grow pentatwinned nanoparticles with different morphologies – bipyramids, nanorods, and decahedra – based on previously reported protocols. For each nanoparticle type, the aspect ratio could be readily tuned by simply varying seed concentration, keeping all other parameters constant. The results are summarized in Figure 3, including UV-Vis-NIR spectra and representative TEM images for a wide range of seed concentrations. It is obvious from the spectra that yields are very high in all cases, even though each sample was obtained in a single growth step and no purification was applied. In the case of bipyramids the Au3+/Au0 ratio was varied between 40 and 8333, leading to dipolar longitudinal LSPR bands ranging from 677 to 1796 nm (Figure 3a), for aspect ratios between 2.44 and 5.22 (length varied from 44.0±1.6 to 585.9±29.7 nm, equatorial width ranged from 18.2±0.8 to 112±10.9 nm) (Figure 3b-e; Figures S10-S14, and Table S1). Gold nanorods were prepared using the well-known silver-free seeded-growth process, originally developed by Murphy18 (using CTAB and ascorbic acid). Again using one-step seeded growth, and varying only the Au3+/Au0 ratio between 100 and 1667, nanorods were readily obtained with aspect rations ranging from 2 to 5 (length: 58.6 ± 0.8 to 236.5 ± 0.9 nm, width from 18.0 ± 1.0 to 34.2 ± 0.3 nm) (Figures 3g-j; Figures S15 - S17, Table S2). High quality LSPR spectra were recorded, with the longitudinal plasmon band red-shifting from 730 up to 1280 nm, as the amount of seeds was decreased (Figure 3f). For both bipyramids and nanorods, additional bands are observed at higher aspect ratios, which correspond to higher order plasmon modes. As a final example, we used the same seeds for the synthesis of gold decahedra.

The experimental conditions were adapted from our recent work 7 , using CTAC and ascorbic acid. For Au3+/Au0 ratios between 36 and 5000, a variation in decahedra side length was obtained from 15.6±0.6 to 79.8 ± 1.0 nm (Figure 3l-o; Figure S18, and Table S3). The LSPR position varied in a much narrower range in this case (541 – 608 nm, Figure 3k), as expected for the lower anisotropy of decahedra, as compared to nanorods and bipyramids.

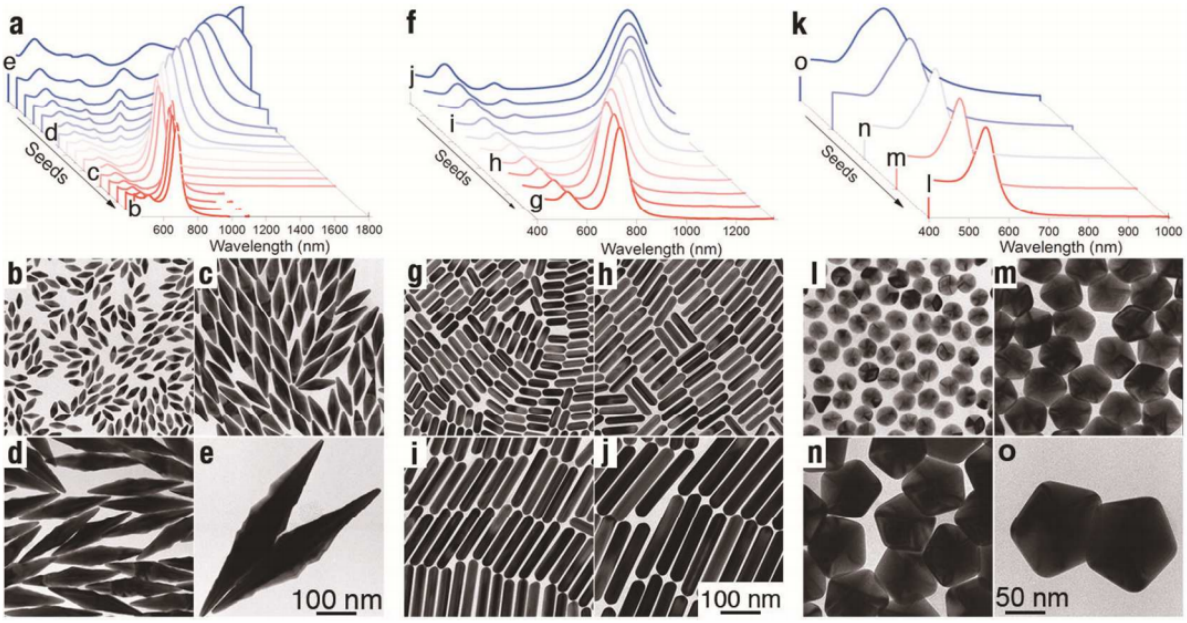

Figure 3. Universal character of thermally-treated seeds. Effect of seed concentration on the growth of bipyramids (a-e), nanorods (f-j) and decahedra (k,o). (a,f,k) UV-Vis-NIR spectra of colloids prepared with different seed concentrations and representative TEM images of nanoparticles prepared in a single growth step from different amounts of seeds.

The high quality of the obtained samples, both in shape yield and monodispersity, as well as the wide range of available dimensions, allowed us to evaluate the relationship between longitudinal LSPR band position and average aspect ratio for both nanorods and bipyramids (Figure S19). Whereas a linear trend was observed for nanorods, in agreement with previous reports,[19,20] bipyramids displayed a double-linear behavior, i.e. two different slopes below and above aspect ratio 4.5. Remarkably, a dramatic red-shift of 800 nm was determined for an aspect ratio increased between 4.5 and 5.2. This large variation is likely related to changes in the volume of the nanoparticles,[10,21] while for nanorods the particle volume varies linearly with aspect ratio, the increase is non-linear for bipyramids (Figure S19). It should however be taken into account that variations in the detailed shape and surface roughness were observed for larger bipyramids, which may be of relevance to their optical response[19] .

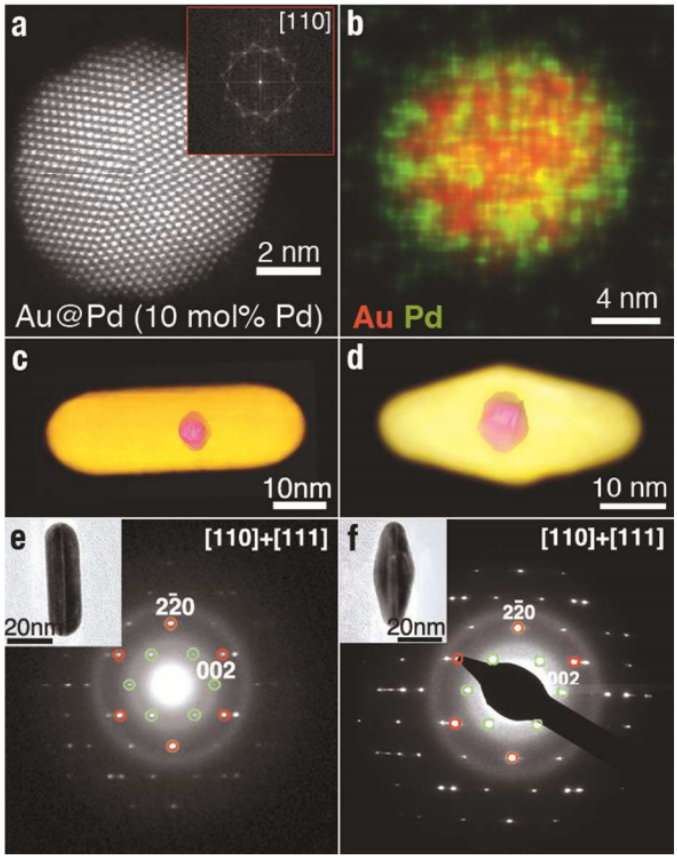

Figure 4. Localization of seeds after growth. (a) HAADF-STEM image of a thermally treated seed overgrown with palladium (10 mol%), preserving the crystal structure. (b) Energy Dispersive Xray Spectroscopy (XEDS) mapping of Au@Pd (10 mol%) showing the outer distribution of Pd. (c, d) 3D visualization of the reconstructed volume of an individual nanorods (c) and bipyramid (d) obtained through the standard growth process using Au/Pd seeds. 10 and 50 mol% Pd for rods and bipyramids, respectively. (e, f) Selected Area Electron Diffraction (SAED) pattern of an individual nanorods (e) and bipyramid (f). The green and red circles indicate the reflections of the [110] and [111] orientations respectively.

Our system additionally offers advantages toward understanding the growth mechanism of anisotropic nanoparticles. In the conventional seeded growth methods, a major difficulty lies on the difficult visualization of seeds within the final particles, because of their small size.[22] The larger size of thermally treated seeds (6 nm) allows us to incorporate a second metal in the seed structure, which can be used as a marker that facilitates visualization by electron microscopy. The most suitable choice for this purpose is palladium, with low atomic mass (106.46u) compared to gold (196.96u), which ensures sufficient contrast for electron microscopy characterization in HAADF-STEM mode. It has been observed that palladium can be reduced as a shell while preserving the crystallinity of the original gold seed (epitaxial growth).[23] We thus deposited different amounts of Pd (10 and 50 mol%) on thermally treated seeds, obtaining a core-shell structure with a slightly larger diameter: 6.1±0.4 nm (10 mol% Pd; see Figures 4b and S20) and 6.2±0.7 nm (50 mol% Pd)[24] (Figure S21). FFT analysis confirmed that the presence of palladium did not alter the structure of seeds (Figure 4a). Seeds with different Pd content were subsequently used to prepare nanorods (AuPd 10 mol%) and bipyramids (AuPd 50 mol%). As can be easily seen in Figure 4, the Au/Pd seeds could be accurately identified within the particles for both morphologies. Interestingly, while for bipyramids (Figures 4d, S22c,d) the seed was typically found near the geometrical center, for nanorods (Figures 4c, S22a,b) we found that the seed was often off center, which raises questions regarding the

symmetry breaking and growth mechanisms. Finally, electron diffraction analysis revealed that, for both bipyramids and rods, the growth direction [110] matches that of the original seeds, as expected for the proposed relationship between the crystal habit of the seeds and that of the particles obtained by seeded growth.

We have shown that a mild thermal treatment of conventional Au seeds in solution results in quasi-quantitative formation of twin planes. The use of twinned particles for seeded-growth under standard conditions largely improves the synthetic yield of bipyramids, nanorods and decahedra, as compared to current protocols, reaching values close to 100%. Our results are expected to greatly advance the generalization of current synthetic methods, upscaling of anisotropic nanoparticle synthesis, and open up new way to investigate growth mechanisms.

ASSOCIATED CONTENT

Supporting Information

The Supporting Information is available free of charge on the ACS Publications website. Experimental details, control experiments, and additional microscopy images (PDF)

AUTHOR INFORMATION

Corresponding Author

mgrzelczak@cicbiomagune.es; llizmarzan@cicbiomagune.es

Funding Sources

Any funds used to support the research of the manuscript should be placed here (per journal style).

ACKNOWLEDGMENT

Financial support is acknowledged from the European Research Council through ERC Advanced Grant Plasmaquo and the ERC Starting Grant COLOURATOM. T.A. acknowledges financial support from the Research Foundation Flanders (FWO, Belgium) through a postdoctoral grant.

REFERENCES

(1) Lohse, S. E.; Murphy, C. J. Chem. Mater. 2013, 25 (8), 1250.

(2) Lim, B.; Xia, Y. Angew. Chem. Int. Ed. 2011, 50 (1), 76.

(3) Gao, C.; Goebl, J.; Yin, Y. J. Mater. Chem. C 2013, 1 (25), 3898.

(4) Personick, M. L.; Mirkin, C. A. J. Am. Chem. Soc. 2013, 135 (49), 18238. Page 4 of 6 ACS Paragon Plus Environment Journal of the American Chemical (5) Ye, X.; Jin, L.; Caglayan, H.; Chen, J.; Xing, G.;

Zheng, C.; Doan-Nguyen, V.; Kang, Y.; Engheta, N.; Kagan, C. R.; Murray, C. B. ACS Nano 2012, 6 (3), 2804.

(6) Langille, M. R.; Personick, M. L.; Zhang, J.; Mirkin, C. A. J. Am. Chem. Soc. 2012, 134 (35), 14542.

(7) Grzelczak, M.; Sánchez-Iglesias, A.; Heidari, H.; Bals, S.; Pastoriza-Santos, I.; Pérez-Juste, J.; Liz-Marzán, L. M. ACS Omega 2016, 1 (2), 177.

(8) Pérez-Juste, J.; Liz-Marzán, L. M.; Carnie, S.; Chan, D. Y. N.; Mulvaney, P. Adv. Funct. Mater. 2004, 14 (6), 571.

(9) Lee, J.-H.; Gibson, K. J.; Chen, G.; Weizmann, Y. Nat Commun 2015, 6, 7571.

(10) Chateau, D.; Liotta, A.; Vadcard, F.; Navarro, J. R. G.; Chaput, F.; Lermé, J.; Lerouge, F.; Parola, S. Nanoscale 2015, 7 (5), 1934.

(11) Liu, M.; Guyot-Sionnest, P. J. Phys. Chem. B 2005, 109 (47), 22192.

(12) Li, Q.; Zhuo, X.; Li, S.; Ruan, Q.; Xu, Q.-H.; Wang, J. Adv. Opt. Mater. 2015, 3 (6), 801.

(13) Guo, Z.; Wan, Y.; Wang, M.; Xu, L.; Lu, X.; Yang, G.; Fang, K.; Gu, N. Colloid Surf. A 2012, 414, 492.

(14) Jana, N. R. Chem. Commun. 2003, No. 15, 1950.

(15) Scarabelli, L.; Sánchez-Iglesias, A.; Pérez-Juste, J.; LizMarzán, L. M. J. Phys. Chem. Lett. 2015, 6 (21), 4270.

(16) Xia, Y.; Xia, X.; Peng, H.-C. J. Am. Chem. Soc. 2015, 137 (25), 7947.

(17) Xiong, Y.; McLellan, J. M.; Yin, Y.; Xia, Y. Angew. Chem. Int. Ed. 2007, 46 (5), 790.

(18) Jana, N. R.; Gearheart, L.; Murphy, C. J. Adv. Mater. 2001, 13 (18), 1389.

(19) Liu, M.; Guyot-Sionnest, P.; Lee, T.-W.; Gray, S. K. Phys. Rev. B 2007, 76 (23), 235428.

(20) Pérez-Juste, J.; Pastoriza-Santos, I.; Liz-Marzán, L. M.; Mulvaney, P. Coord. Chem. Rev. 2005, 249 (17–18), 1870.

(21) Kou, X.; Ni, W.; Tsung, C.-K.; Chan, K.; Lin, H.-Q.; Stucky, G. D.; Wang, J. Small 2007, 3 (12), 2103.

(22) Langille, M. R.; Zhang, J.; Personick, M. L.; Li, S.; Mirkin, C. A. Science 2012, 337 (6097), 954.

(23) Fan, F.-R.; Liu, D.-Y.; Wu, Y.-F.; Duan, S.; Xie, Z.-X.; Jiang, Z.-Y.; Tian, Z.-Q. J. Am. Chem. Soc. 2008, 130 (22), 6949.

(24) Grzelczak, M.; Pérez-Juste, J.; Rodríguez-Fernández, B.; Liz-Marzán, L. M. J. Mater. Chem. 2006, 16 (40), 3946.